Development 123, 357-367
Printed in Great Britain © The Company of Biologists Limited 1996
DEV3324

Mutations affecting craniofacial development in zebrafish

Stephan C. F. Neuhauss, Lilianna Solnica-Krezel*, Alexander F. Schier, Fried Zwartkruis†, Derek L. Stemple, Jarema Malicki, Salim Abdelilah, Didier Y. R. Stainier‡ and Wolfgang Driever§

Cardiovascular Research Center, Massachusetts General Hospital and Harvard Medical School, 149 13th Street, Charlestown, MA 02129, USA

*Present address: Department of Molecular Biology, Vanderbilt University, Box 1820, Station B, Nashville, TN 37235
†Present address: Laboratory for Physiological Chemistry, Utrecht University, Universiteitsweg 100, 3854 CG Utrecht, The Netherlands
‡Present address: School of Medicine, Department of Biochemistry and Biophysics, UCSF, San Francisco, CA 94143-0554, USA
§Author for correspondence (e-mail: driever@helix.mgh.harvard.edu)

SUMMARY

In a large-scale screen for mutations affecting embryogenesis in zebrafish, we identified 48 mutations in 34 genetic loci specifically affecting craniofacial development. Mutants were analyzed for abnormalities in the cartilaginous head skeleton. Further, the expression of marker genes was studied to investigate potential abnormalities in mutant rhombencephalon, neural crest, and pharyngeal endoderm. The results suggest that the identified mutations affect three distinct aspects of craniofacial development. In one group, mutations affect the overall pattern of the craniofacial skeleton, suggesting that the genes are involved in the specification of these elements. Another large group of mutations affects differentiation and morphogenesis of cartilage, and may provide insight into the genetic control of chondrogenesis. The last group of mutations leads to the abnormal arrangement of skeletal elements and may uncover important tissue-tissue interactions underlying jaw development.

Key words: *Danio rerio*, craniofacial mutants, cartilage, pharyngeal arches

INTRODUCTION

The head skeleton in vertebrates mainly comprises derivatives of the cranial neural crest, a transient migratory population of cells unique to vertebrates (Noden, 1983, 1975; Le Lievre, 1978; Couly et al., 1993). During closure of the neural tube, the cranial neural crest cells migrate from the dorsal aspect of the neural tube into the frontonasal process and the pharyngeal arches. Cranial neural crest derivatives include a large part of the head skeleton, dermis of the face, most of the skull, some neurons and glia of several cranial ganglia, and Schwann cells of the cranial nerves (Le Douarin, 1982). Cranial neural crest cells appear to migrate according to their rhombomeric origin (Lumsden et al., 1991). For example, cells from rhombomere 2 migrate to the first pharyngeal (mandibular) arch, whereas cells from rhombomere 4 migrate into the second pharyngeal (hyoid) arch. Transplantation experiments indicate, that cranial crest cells may be determined before the onset of migration (Noden, 1983).

After the pharyngeal arches become populated with neural crest-derived cells, chondrogenesis can be first observed as mesenchymal, neural crest-derived cells undergo condensation. The pharyngeal endoderm has been identified as necessary for the induction of cartilage formation (Graveson and Armstrong, 1987; Seufert and Hall, 1990). Most of the cartilage formed by neural crest-derived cells is subsequently replaced by osteoblasts during bone formation.

While more recent studies of craniofacial development have focused on chick and mouse embryos, similar conclusions regarding craniofacial development have been obtained in lower vertebrates, such as teleosts (Langille and Hall, 1987, 1988; Schilling, 1993; Miyake and Hall, 1994). In the zebrafish, *Danio rerio*, anterior cranial neural crest cells start to emigrate around intermediate segmentation stages, followed shortly by cells of progressively more caudal levels. Those cells migrate ventrally, subsequently forming a reiterated series of seven pharyngeal arch primordia separated by endodermal epithelial pouches. Labeling studies suggest that arch precursors are fated near the onset of migration and produce clones confined to single arches and probably single cell types. Furthermore, the fate of these cells can be predicted by their position within the precursor populations. The chondrogenic neural crest cells are the most medial and the last to emigrate. By 72 hours post fertilization (hpf), many of the neural crest-derived mesenchymal cells have differentiated into long rows of cartilage within each arch making up the pharyngeal skeleton (Schilling, 1993; Schilling and Kimmel, 1994).

Most of our understanding of craniofacial development stems from embryological experiments. Mutational analyses in mice have provided new insights. Skeletal development can be disrupted by mutations at several steps in the pathway. Defects in the patterning of the head skeleton have been described for mice carrying mutations in several of the Hox genes (Chisaka and Capecchi, 1991; Gendron-Maguire et al., 1993; Rijli et al., 1993). Several mutations, such as *short ear* and *brachypodism*, both of which encode growth factors of the TGFβ superfam-

ily affect the formation of the mesenchymal condensations (Kingsley et al., 1992; Storm et al., 1994).

Recently, conditions for efficient recovery of mutations in zebrafish have been described (Mullins et al., 1994; Solnica-Krezel et al., 1994). We have used a genetic approach to study craniofacial development in zebrafish. In a genome-wide large scale screen for mutations with abnormal embryogenesis (Driever et al., 1996), we have identified mutations in 34 genetic loci affecting specific aspects of craniofacial development. We analyzed the pharyngeal skeleton of the mutants at a morphological level using a stain for proteoglycans. For several mutations we also investigated the organization of the rhombencephalon and the pharyngeal arch primordia for alteration of the expression pattern of marker genes.

Our results suggest that the identified mutations can be categorized into three groups. (1) Mutations affecting the layout of the pharyngeal skeleton. These mutations are characterized by absence or displacement of individual elements of the pharyngeal skeleton. (2) Mutations affecting the differentiation and morphogenesis of cartilaginous skeletal elements and (3) mutations affecting the spatial arrangement of normally formed pharyngeal skeletal elements.

MATERIALS AND METHODS

Mutations were induced by the alkylating mutagen N-ethyl-N-nitrosurea (ENU) and recovered in an F_2 screen as previously described (Solnica-Krezel et al., 1994; Driever et al., 1996) All embryos were maintained at 28.5°C and staged according to development in hours (hpf) or days (dpf) postfertilization.

Phenotypic analysis

Larvae were anesthetized in 0.02% buffered 3-aminobenzoic acid methyl ester (Sigma) and observed under a dissecting microscope. Embryos were embedded in 2% methylcellulose and photographed either under a dissecting scope or using differential interference contrast (DIC) optics on a Zeiss Axiophot microscope (Westerfield, 1994).

Cartilage was stained with Alcian blue, using a modified protocol of Kelly and Bryden (1983). Larvae at 5 dpf or older were fixed overnight in 4% phosphate-buffered paraformaldehyde and washed several times in phosphate-buffered saline with 0.1% Tween-20 (PBT). In order to enhance their optical clarity, the specimens were bleached in 30% hydrogen peroxide for 2 hours or until the eyes were sufficiently translucent. The embryos were rinsed in PBT and transferred into a filtered, Alcian blue solution (1% concentrated hydrochloric acid, 70% ethanol, 0.1% Alcian blue) and stained overnight. Specimens were cleared in acidic ethanol (5% concentrated hydrochloric acid, 70% ethanol) for 4 hours, dehydrated in an ethanol series and stored in glycerol. Specimens were analyzed and documented in glycerol under epillumination on a dissecting microscope.

Whole-mount in situ hybridization was performed with digoxigenin-labeled RNA probes essentially as described by Oxtoby and Jowett (1993). Embryos were scored in PBT and documented after clearing in benzylbenzoate/benzyl alcohol (2:1). The following probes were used: *krx-20* (Oxtoby and Jowett, 1993), *pax 2* (Krauss et al., 1991), *hlx-1* (Fjose et al., 1994), *dlx-2*, *dlx-3* and *dlx-4* (Ekker et al., 1992; Akimenko et al., 1994).

Immunocytochemistry with the monoclonal antibody zn-5 (Trevarrow et al., 1990) was performed on early pharyngula embryos (24 -28 hpf) after fixation in 4% paraformaldehyde (4 hours at room temperature). Subsequent steps were performed essentially as previously described (Solnica-Krezel and Driever, 1994). Hybridoma supernatant was used at a 1:5 dilution.

For metacrylate sections, larvae were fixed overnight in 4% paraformaldehyde (4°C, overnight) and dehydrated in ethanol, then embedded in JB-4 resin, according to the manufacturer's instructions (Polyscience Inc.). Sections (5 μm) were cut on a Leica 2065 microtome.

Genetic analysis

Genetic segregation of individual mutations was determined by assessing on average 1000 embryos from crosses of heterozygous parents for any given mutation. In order to test potential allelism of isolated mutations, complementation testing among members of the phenotypically defined groups of mutations was performed. Complementation between two mutations was tested by crossing identified heterozygous parents of each mutation and screening their offspring for the mutant phenotype. A minimum of 30 embryos per complementation cross was analyzed. If all embryos developed as wild-type, mutations were considered to be in distinct loci. If about 25% of the embryos develop the mutant phenotype, they were considered to be allelic. All mutations segregate as Mendelian recessive traits. A total of 278 successful complementation crosses were performed with 14,886 embryos scored.

Heterozygous parents of mutant embryos were outcrossed and the heterozygotes were reidentified in sibling incrosses.

RESULTS

The pharyngeal skeleton of 5-day old zebrafish larvae

The pharyngeal skeleton of the zebrafish consists of 7 pharyngeal (visceral) arches with the anterior two forming jaw and the posterior five forming gill structures.

After 3 dpf the cartilage of the pharyngeal skeleton of all 5 gill arches can be stained with Alcian blue. In a 5 dpf larva, individual components of the pharyngeal skeleton can be reliably identified (Fig. 1). By analogy to other vertebrates, the pharyngeal arch from which individual components derive can be assigned (De Beer, 1937; Langille and Hall, 1987; Miyake and Hall, 1994). The first pharyngeal (mandibular) arch derivatives are: Meckel's cartilage and the quadrate with the pterygoid process. Second pharyngeal (hyoid) arch derivatives include the ceratohyal, the hyosymplectic, the interhyal and the basihyal. The third to seventh pharyngeal arch (first to fifth gill arch derivatives) include the basibranchial, the ceratobranchials and hypobranchials. Also visible are the trabeculae of the chondrocranium, which are fused to form the ethmoid plate. The zebrafish pharyngeal skeleton develops in a way similar to that of other teleosts, e.g. *Salmo salar* (De Beer, 1937) and *Oryzias latipes* (Langille and Hall, 1987).

Identification of mutations affecting craniofacial development

Mutations affecting craniofacial development were identified in an F_2 screen as described by Driever et al. (1996). Zebrafish larvae were screened by visual inspection under the dissecting microscope. Abnormalities in the jaw and gill structures can be detected best at 5 dpf. Two major categories of abnormal craniofacial phenotypes were formed.

The first category comprise mutations that lead to reduced craniofacial differentiation accompanied by overall delay of development. This syndrome manifests itself by a general delay in growth made apparent by small eye size, reduced body length and smaller pectoral fins and was observed in 24%

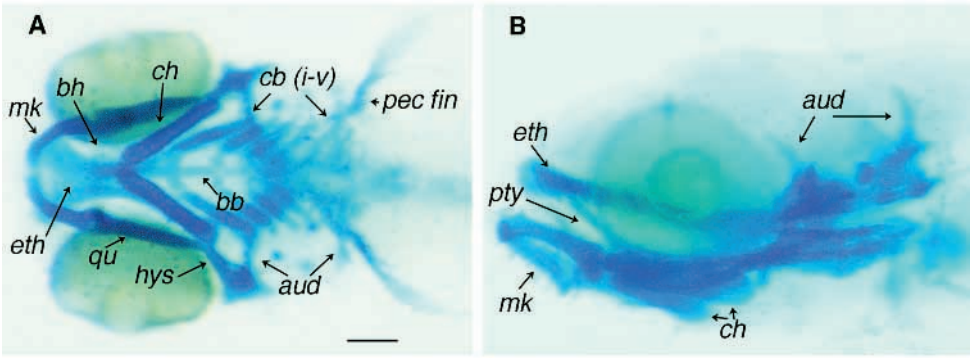

Fig. 1. Pharyngeal skeleton of a day-5 zebrafish larva stained for cartilage with Alcian blue. (A) Ventral view. Individual cartilaginous elements of the pharyngeal skeleton are identifiable. The two trabeculae fuse medially to form the ethmoid plate (eth). First arch derivatives are Meckel's cartilage (mk) and quadrate (qu). Second arch derivatives are basihyal (bh), ceratohyal (ch), hyosymplectic (hys). Gill arch derivatives are basibranchials (bb) and ceratobranchials I-V (cb i-v). Also labeled are cartilages of the pectoral fins (pec fin). (B) Lateral view reveals the pterygoid process of the quadrate (pty) and the auditory capsule (aud). Scale bar is 100 μm.

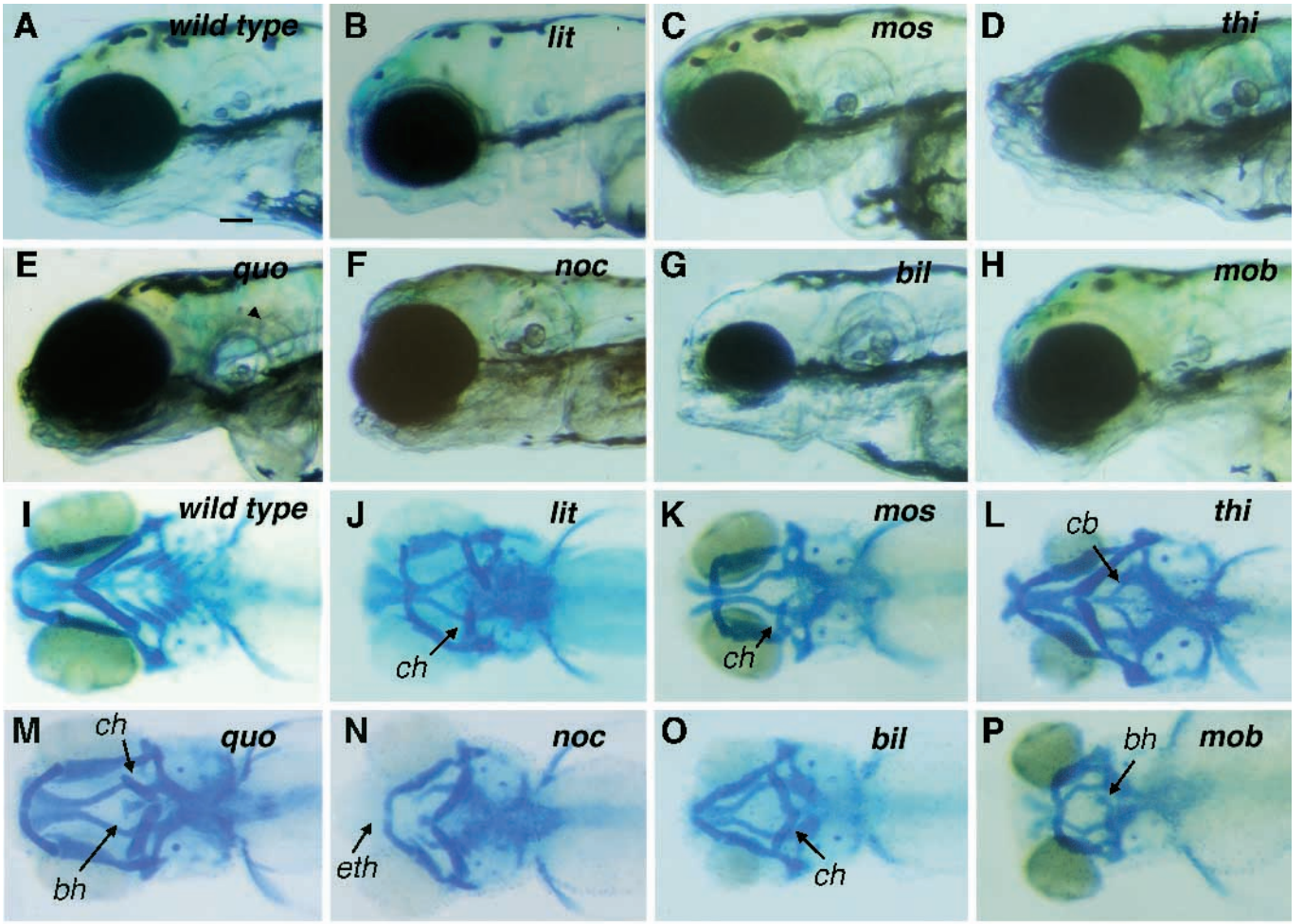

Fig. 2. Mutations affecting the layout of the pharyngeal skeleton. (A-H) Lateral view of a living day-5 larvae. (I-P) Ventral view of Alcian blue stained larvae. (A,I) Wild-type embryos. (B,J) *little richard*^{m433}. (C,K) *mother superior*^{m188}. (D,L) *thinner*^{m214}. (E,M) *quadro*^{m271}. (F,N) *nocyrano*^{m579}. (G,O) *bielak*^{m429}. (H,P) *mont blanc*^{m610}. For details, see text. wt, wild-type; bh, basihyal; cb, ceratobranchial; ch, ceratohyal; and eth, ethmoid plate. Scale bar, 100 μm.

(587/2383) of all embryonic and early larval lethal mutations found in the screen. These pleiotropic mutations appear to cause a non-specific general delay in development, possibly due to some metabolic defect, and may not be involved specifically in craniofacial development. We excluded these mutations from further analysis. A sample of 16 independent mutations leading to such phenotypes were subjected to skeletal analysis. All but one had a craniofacial phenotype consistent with a general delay in development. The entire pharyngeal skeleton was found to be properly formed and differentiated but was reduced in size. In only one isolate did the ceratohyal not reach the midline (Fig. 7F).

The second category includes mutations that affect specific aspects of craniofacial development. We recovered 48 independent mutations and each was subjected to further phenotypic and genetic characterization.

The nature of the defects observed allowed us to classify these mutants into three groups: (1) mutations affecting the layout of the pharyngeal skeleton; (2) mutations affecting the differentiation and morphogenesis of cartilaginous elements of the pharyngeal skeleton; and (3) mutations affecting the spatial arrangement of normally formed skeletal elements. Several other mutations presented in this manuscript do not fit into these categories, but appear also to affect specific aspects of craniofacial development.

Complementation analysis was performed within each group. The 48 isolated mutations fall into 34 complementation groups. Table 1 presents a brief summary, including phenotypic aspects not related to craniofacial development.

Group I: Mutations affecting the layout of the pharyngeal skeleton

Alcian blue staining produced evidence of the absence or displacement of individual elements of the pharyngeal skeleton for 9 mutations in 7 loci. All of the mutations are early larval lethal, meaning that they hatch as free swimming larvae but do not inflate their swim bladder and are unable to feed.

Mutant *little richard* (*lit*) alleles (*m181* and *m433*) cause a severe reduction of the jaw and gill apparatus (Fig. 2B,J). Meckel's cartilage and quadrate are reduced both in size and rostral extent. The ceratohyal is bent caudally and is smaller. The basihyal and hyosymplectic cartilage are present but are smaller and positioned more caudally. In the majority of homozygous mutant embryos only the first two and the fifth ceratobranchials are detectable. In a few cases the third ceratobranchial is visible. The two alleles produce similar jaw phenotypes but differ in other aspects. In lit^{m433} mutants at 2 dpf the auditory vesicle is much smaller and does not form semicircular canals. Most homozygous mutant embryos in this group have cardiac edema and reduced circulation due to malformations of the atrioventricular valve. In contrast, homozygous lit^{m181} mutants have normal circulation and only a slightly smaller auditory capsule. The pharyngeal arches are populated slightly later by *dlx*-positive cells (see below).

The *mother superior* (mos^{m188}) mutation leads to a severe reduction of the pharyngeal skeleton sometimes accompanied by a ventral displacement of Meckel's cartilage (Fig 2C,K). Skeletal analysis reveals the absence of the basihyal and no detectable ceratobranchials with the occasional exception of ceratobranchial V. The hyosymplectic and the ceratohyal are missing or reduced in the majority of embryos. In about half of the mutant embryos the trabeculae are not fused, so that the ethmoid plate is not formed.

Most *thinner* (thi^{m214}) mutant embryos develop only the first and the fifth ceratobranchial, while some have none or up to three visible ceratobranchials (Fig. 2D,L). All lower jaw structures are reduced in their rostral extent, whereas the ethmoid plate is only slightly smaller.

Skeletal analysis of *quadro* (quo^{m271}) mutant embryos reveals that the rostral extent of the basihyal and the gill arches is reduced (Fig. 2E,M). The ceratohyal is shorter and deflected caudally. In a few embryos one of the ceratohyals extends over the midline. The hyosymplectic is much smaller and sometimes not detectable. The ceratobranchials are reduced in number with the majority of embryos developing only three. The entire gill arch complex is shifted caudally and the ceratobranchials are bent caudally rather than dorsally. Malformations of the auditory capsule are not necessarily bilaterally symmetric and range from very small empty auditory capsules to duplications of well-formed ears.

For *nocyrano* (noc^{m579}) the majority of mutant embryos have trabeculae that are not fused to form the ethmoid plate, and are not connected to the basal plate (Fig. 2F,N). In some embryos the trabeculae are only weakly stained or not visible at all. The lower jaw is slightly delayed in its formation. Meckel's cartilage is dorsally bent in relation to the quadrate, reminiscent of the hai^{m114} and $rochen^{m193}$ phenotype (Fig. 6C,D).

In homozygous *bielak* (bil^{m429}) embryos, the ethmoid plate, as well as Meckel's cartilage, quadrate, ceratohyal and hyosymplectic are smaller (Fig. 2G,O). The ceratohyal points caudally. While the first and the fifth ceratobranchials are visible in all mutant embryos, the second ceratobranchial is rarely present and the other ones are not detectable.

In mutant embryos of two indistinguishable *mont blanc* (*mob*) alleles (*m610* and *m780*), all skeletal elements of the head are smaller (Fig. 2H,P). Meckel's cartilage, quadrate and basihyal are reduced both in size and rostral extent. In about half of the mutant embryos the basihyal is laterally displaced from its medial position. Ceratohyal and hyosymplectic are very small and do not extend toward the midline or are not detectable. The trabeculae are thinner, reduced in their rostral extent and do not fuse. The ceratobranchials are not visible with the rare exception of very small first and fifth ceratobranchials.

To determine whether the observed phenotypes correlate with patterning defects in the rhombencephalon, the expression of *krx-20*, *pax b* and *hlx-1* was analyzed in mutant embryos for each locus of this group. The expression patterns of *krx-20* (Oxtoby and Jowett, 1993) and *pax b* (Krauss et al., 1991) were analyzed at early segmentation stages (12-15 hpf), to assess the anterior-posterior patterning of the rhombencephalon. These genes are expressed in rhombomere 3 and 5, and in the midbrain, respectively. At early pharyngula stages (24-28 hpf) *hlx-1* (Fjose et al., 1994) is expressed in paired stripes in all rhombomeres. The expression pattern of these three genes indicates no abnormalities in the rhombencephalon organization for any of the mutants in this group. Antibody staining using zn-5 (Trevarrow et al., 1990), a monoclonal antibody which labels the endodermal pouches of the pharyngeal arches, revealed no structural abnormalities in mutant embryos (data not shown).

To detect abnormalities in the formation of the pharyngeal arches we analyzed the expression of *dlx-2*, *dlx-3* and *dlx-4* (Ekker et al., 1992; Akimenko et al., 1994) at early pharyngula stages (24-28 hpf). These markers are expressed in a combinatorial fashion in the pharyngeal arch primordia (Akimenko et al., 1994). For mutants affected in lit^{m433} and mos^{m188} the expression of *dlx* genes in the pharyngeal arches is slightly delayed. whereas no difference between mutant and wild-type embryos could be detected for the other loci.

Group II: Mutations affecting cartilage differentiation and morphogenesis

Cartilage differentiation and morphogenesis appear to be

Table 1. Summary of the phenotypes

Genetic loci	Alleles	Craniofacial defect	Other phenotypes	Refs
Group I				
little richard (*lit*)	*m181, m433*	Reduced number of CB	Reduction of otic capsule, reduced circulation (in *m433*)	c
mother superior (*mos*)	*m188*	Absence or reduction of CH, absence of BH and fewer or none CB	Smaller eyes, slightly reduced pigmentation, supernumerary , neuromast organs in trunk	
thinner (*thi*)	*m214*	Reduced number of CB	Smaller eyes	
quadro (*quo*)	*m271*	Reduced and deflected CH, HYS, reduced number of CB	Variable ear malformations (reductions and duplications)	c
bielak (*bil*)	*m429*	Reduction of mandibular and hyoid structures, absence or fewer CB	Lack of xanthophores, fewer and smaller iridiophores, smaller eyes	
mont blanc (*mob*)	*m610, m780*	CH, HYS reduced or not detectable, fewer CB or not detectable	Slightly reduced pigmentation and eye size	
nocyrano (*noc*)	*m579*	ETH not formed, trabeculae not fused with basal plate or absent		
Group II				
bulldog (*bul*)	*m137, m421, m494, m606, m757*	Cartilage growth and differentiation, semicircular canals of inner ear fail to form	Kinked and shorter pectoral fin, fin degeneration	
jekyll (*jek*)	*m151, m310*	Cartilage differentiation affected, no staining with Alcian blue, semicircular canals of inner ear fail to form	Kinked and shorter pectoral fin, atrio-ventricular valve formation	d
mr hyde (*hyd*)	*m205*	Cartilage growth and differentiation, semicircular canals of inner ear fail to form	Kinked and shorter pectoral fin, fin degeneration	
round (*rnd*)	*m211, m641, m713, m715*	Cartilage growth and differentiation, semicircular canals of inner ear fail to form	Kinked and shorter pectoral fin, fin degeneration	
crusher (*cru*)	*m299*	Cartilage growth and differentiation, semicircular canals of inner ear fail to form	Shorter pectoral fin	
zhivago (*zhi*)	*m315*	Cartilage growth and differentiation, semicircular canals of inner ear fail to form	Shorter pectoral fin	
stumpf (*stp*)	*m365*	Cartilage growth and differentiation	Shorter pectoral fin	
strangelove (*stn*)	*m617*	Cartilage growth and differentiation, semicircular canals of inner ear fail to form	Shorter pectoral fin	
feelgood (*fel*)	*m662*	Cartilage growth and differentiation, semicircular canals of inner ear fail to form	Shorter pectoral fin	
apparatchik (*apa*)	*m364*	Pharyngeal skeleton reduced, CH and QU thicker and shorter	Pectoral fins slightly shorter	
rieux (*rix*)	*m526*	Pharyngeal skeleton reduced, CH and QU thicker and shorter	Pectoral fins slightly shorter	
kimble (*kim*)	*m533*	Pharyngeal skeleton reduced, CH and QU thicker and shorter, semicircular canals of inner ear fail to form	Pectoral fins slightly shorter	
postdoc (*pos*)	*m485*	Pharyngeal skeleton reduced, CH bend caudally	Pectoral fins kinked and very reduced in size	
Group III				
long jaw (*ljw*)	*m82*	Ventral displacement of MK		
spitzmaul (*sil*)	*m636*	Ventral displacement of MK		
degenerator (*deg*)	*m412*	Ventral displacement of MK	Tectal degeneration	
the boss (*tbo*)	*m182*	Ventral displacement of MK		
doolittle (*doo*)	*m239*	Ventral displacement of MK, CH collapsed		
rochen (*roh*)	*m193*	Dorsal displacement of MK	Head appears flat, smaller eyes	
hai (*hai*)	*m114*	Dorsal displacement of MK	Head appears flat, smaller eyes	
flycatcher (*flc*)	*m370*	BH and BB displaced ventrally	Smaller eyes	
pelican (*pel*)	*m202, m207*	BH and BB displaced ventrally		
grossmaul (*gro*)	*m643, m752*	BH and BB displaced ventrally		
Others				
brak (*brk*)	*m452*	Bending of individual skeletal elements	Severe reduction of melanocytes and lack of eye pigmentation	
maggot (*mgt*)	*m350, m503, m635*	Cartilage growth and differentiation	Notochord	b
captain hook (*cpt*)	*m169*	ETH absent, compressed lower jaw	Gastrulation	a
white bread (*wib*)	*m384*	Reduced lower jaw, no stained CB	Lack of xantho- and iridiophores, smaller eyes	

BB, basibranchial; BH, basihyal; CB; ceratobranchial(s); CH; ceratohyal; ETH; ethmoid plate; MK, Meckel's cartilage and QU, quadrate. See also Fig. 1. Other phenotypic aspects of these mutants are described by: a, Solnica-Krezel et al., 1996; b, Stemple et al., 1996; c, Malicki et al., 1996; d, Stainier et al., 1996.

defective for all elements of the craniofacial skeleton for 21 mutations in 13 loci (Table 1). These mutations were initially recovered in the visual screen by virtue of a common set of phenotypes characterized by a reduction in body length and a shortened head with craniofacial elements not projecting beyond the eyes (Fig. 3A,C,D).

All mutations in this group cause reduction in the size of the pharyngeal skeleton and most fail to form proper projections

in the inner ear after initial outpocketing. Therefore the semicircular canals of the inner ear are not formed. The intensity of Alcian blue staining in the mutants is generally lower than in their wild-type siblings. The skeletal elements, pectoral fins and the auditory capsule are similarly affected.

Since the pharyngeal endoderm is implicated in tissue interactions necessary for chondrogenesis (Graveson and Armstrong, 1987; Seufert and Hall, 1990), we have analyzed the endodermal pouches of the pharyngeal endoderm in these mutants. Staining with the monoclonal antibody zn-5 revealed no abnormalities in the formation of the endodermal pouches in any of the mutants in this group (data no shown).

All the alleles of *bulldog* (*bul*) – *m137*, *m421*, *m494*, *m606*, *m757* – and *round* (*rnd*) – *m211*, *m641*, *m731*, *m715* – as well as *mr hyde*(*hyd*^{m205}) and *crusher*(*cru*^{m299}) result in the outline of the cartilage rods being poorly defined at 5 dpf (Fig. 3E-H). The auditory capsule is reduced in size and the semi-circular canals do not form (Fig. 4). The chondrocytes do not reach their full size and the amount and density of the extracellular matrix seems to be reduced as judged from sectioned material. We have also analyzed older embryos to detect a potential delay in differentiation. The phenotype remains the same at 8 dpf, which argues against a general delay. The cartilage cells in the pectoral fins are similarly affected.

Embryos mutant at the *jekyll* locus (*m151*, *m310*) are characterized by very weak or absent staining with Alcian blue (Fig. 3I). Use of DIC optics and histological sections reveal that the cartilage in the head is present but smaller and does not stain with Alcian blue (Fig 5). The pharyngeal skeleton is reduced to an extent similar to that of *bul*, *rnd*, *hyd* and *cru* mutants.

Mutants in *zhivago*^{m315}, *stumpf*^{m365}, *strangelove*^{m617} and *feelgood*^{m662} are less severely affected as judged by Alcian blue stain intensity (Fig. 3J-M). Pectoral fins are only slightly reduced in size and not kinked. The phenotype remains the same from 5 to 10 dpf for *strangelove*^{m617} and *feelgood*^{m662}

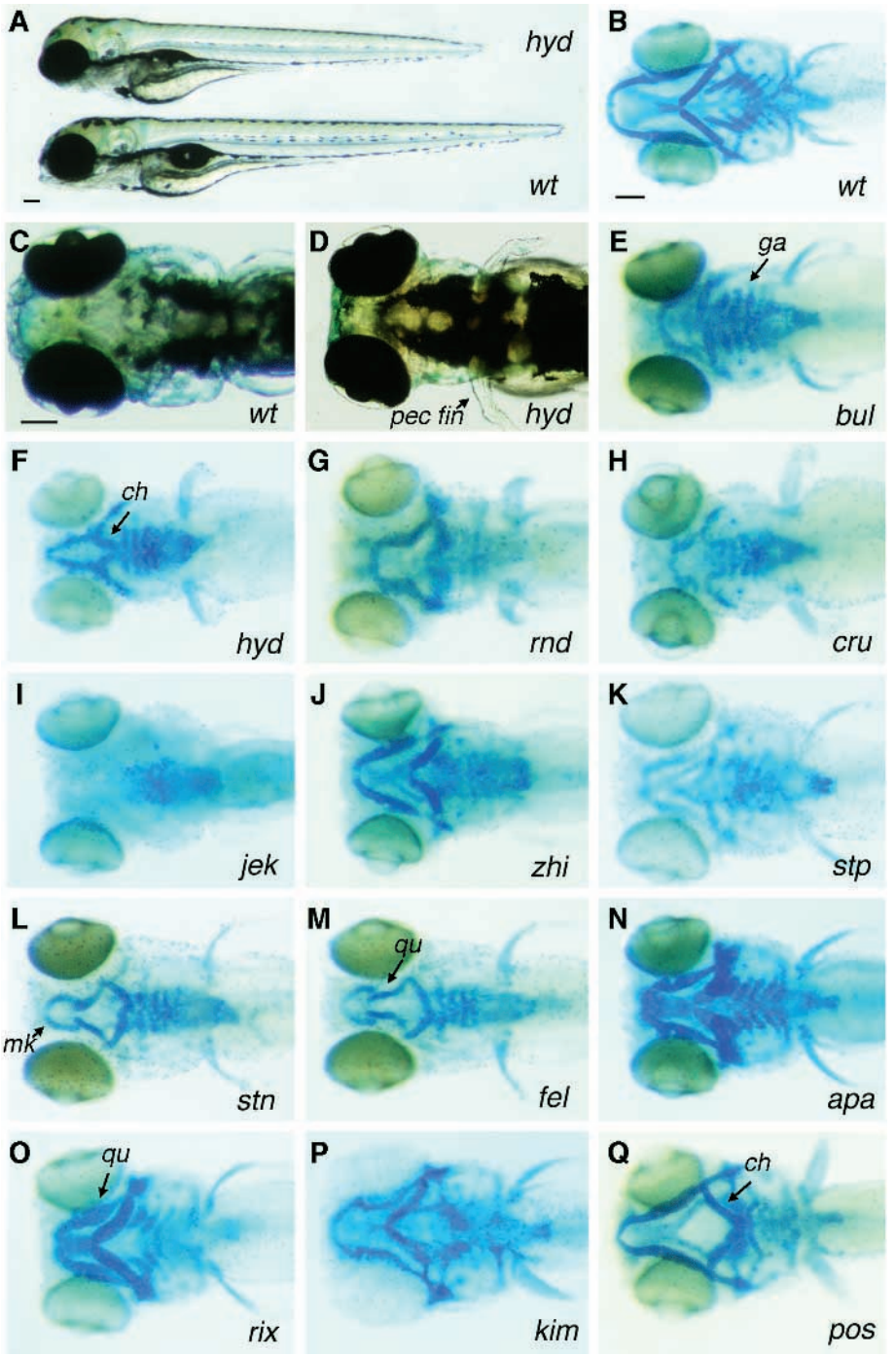

Fig. 3. Mutations affecting chondrogenesis. (A) Mutants are shorter and have reduced jaw structures. Wild-type (bottom) and mutant *mr hyde*^{205} larva (top) at day 5 of development. The mutant is shorter and has a reduced jaw. Wild-type embryos have an inflated swim bladder. (C) Dorsal view of wild-type day-5 larva. (D) Dorsal view of a day-5 *mr hyde*^{205} larva. Notice the rostral position of the eyes and the smaller and bent pectoral fins. (B,E-Q). Ventral views of Alcian blue stained larvae at day 5 of development. (B) Wild-type larva. (E-M) Mutant larvae defective in cartilage formation. Skeletal elements appear smaller and are weakly stained. (E) *bulldog*^{494}, the ceratobranchials are present but smaller; (F) *mr hyde*^{m205}; (G) *round*$^{m713;}$ (H) *crusher*^{m299}; (I) *jekyll*^{m151}; (J) *zhivago*^{m315}; (K) *stumpf*^{m365}; (L) *strangelove*^{m617} and (M) *feelgood*$^{m662.}$ N-Q depict mutant larvae that display stunted growth of skeletal elements. (N) *apparatchik* $^{m364;}$ (O) *rieux*^{m526} (notice the thicker and shorter ceratohyal) and (P) *kimble*^{m533}. (Q) In *postdoc*^{m485} the pharyngeal skeleton is reduced and the ceratohyal is bent ventrally. The pectoral fin is reduced. wt, wild-type; ch, ceratohyal; cb, ceratobranchials; mk, Meckel's cartilage; pec fin; pectoral fin and qu, quadrate. Scale bars, 100 μm.

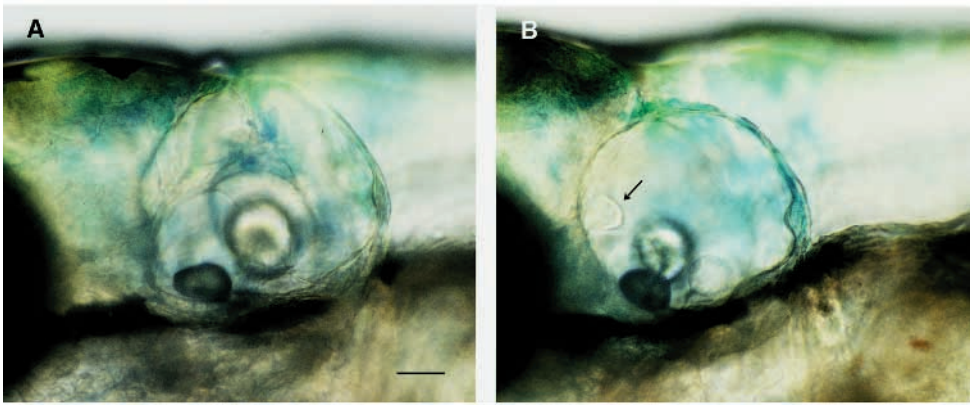

Fig. 4. Lateral view of the ear at day 6 of development. (A) In the wild-type the semicircular canals can be seen. (B) Ear of a *jekyll*^{m151} larva. The epithelial projections are formed but do not elongate and fail to form the semicircular canals. Arrow points to the cranial projection. Scale bar 50 μm.

larvae. With the exception of *stumpf*^{m365} embryos the semicircular canals fail to form.

In *apparatchik*^{m364}, *rieux*^{m526} and *kimble*^{m533} cartilage elements are smaller but stain normally (Fig. 3N-P). The quadrate and ceratohyal appear to be thicker and slightly misshapen. In *kimble*^{m533} the semicircular canals of the inner ear do not form.

In *postdoc*^{m485} the cartilage is quite normal, but the individual cartilage bars are reduced in size (Fig. 3Q). The ceratohyal is bent caudally and the ceratobranchials are smaller. In some mutant embryos the ceratobranchials are fused into a loosely packed mass of cartilaginous cells. As for the other members of this group, the pectoral fins are very reduced in size and the embryos are shorter.

Group III: Mutations affecting the spatial arrangement of pharyngeal skeletal elements

For 12 mutations defining 10 genetic loci cartilaginous elements form normally but are perturbed in their spatial arrangement (Table 1). A ventral view of a mutant head skeleton reveals no difference from the pattern of wild-type siblings. Only observation from a lateral perspective allows identification of the mutant phenotypes (Fig. 6). Some mutants cause a ventral bend of the cartilage rod formed by the basihyal

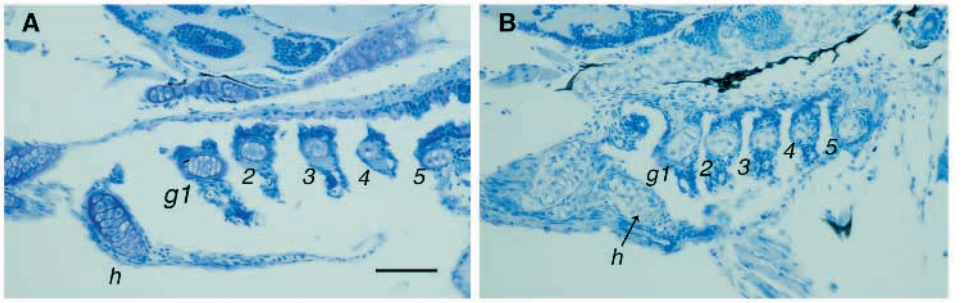

Fig. 5. Sagittal sections of the gill arch region of day-5 larvae. Sections were stained with methylene blue. (A) Wild-type. (B) *jekyll*^{m151}. Notice that the whole gill region is more compressed and that there is a lack of purple staining surrounding the cartilage cells. h, hyoid arch; g1-5, gill arches. Scale bar, 50 μm.

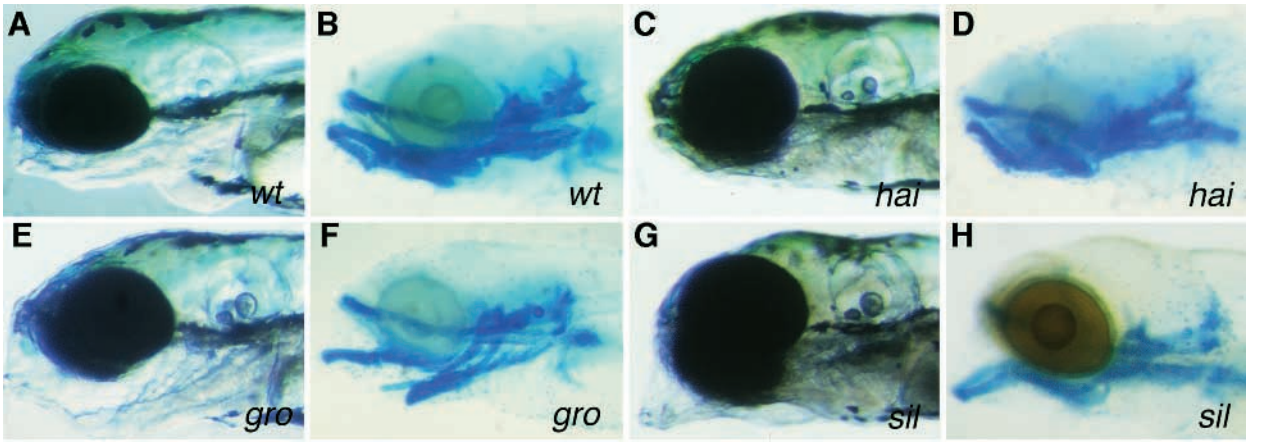

Fig. 6. Mutations affecting the spatial relationship between elements of the pharyngeal skeleton. Lateral view of live day-5 larvae (A,C,E,G) and their corresponding Alcian blue staining (B,D,F,H). (A,B) Wild type (wt). (C,D) *hai*^{m114}. (E,F) *grossmaul* ^{m643}. (G,H) *spitzmaul*^{m636}. For details see text. Scale bar, 100 μm.

and the basibranchials, which results in a gaping jaw. The other mutations result in an abnormal angle between Meckel's cartilage and the quadrate.

Mutant *hai*^{m114} and *rochen*^{m193} larvae are characterized by a dorsal displacement of Meckel's cartilage in relation to the quadrate (Fig. 6C,D). Therefore the jaw appears to be shorter. This is not due to a reduction in size of any element of the jaw apparatus but rather to the reduced angle between Meckel's cartilage and the quadrate.

Embryos mutant in *long jaw*^{m82}, *spitzmaul*^{m636}, *the boss*^{m182}, *degenerator*^{m412} and *doolittle*^{m239} loci were initially identified due to an apparently elongated lower jaw. Further skeletal analysis indicated that the angle between Meckel's cartilage and the quadrate is altered due to a ventral displacement of Meckel's cartilage (Fig. 6G,H). Therefore the rostral extent of the lower jaw is increased. In addition, the ceratohyal is displaced ventrally in *doolittle*^{m239}. Some embryos homozygous for *long jaw* ^{m82} and *spitzmaul*^{m636} form an inflated swim bladder by 5 dpf and are therefore not considered to be early larval lethal. No attempt was undertaken to raise these fish to later larval stages or adulthood.

Alleles of *pelican* (*m202, m207*) and *grossmaul* (*m643, m752*) have been identified because they lead to a gaping jaw phenotype. Skeletal analysis reveals that the cartilage rod formed by the basihyal and the basibranchials is bent ventrally (Fig, 6E,F). The extent of jaw gaping is variable. Some of the homozygous mutant embryos develop inflated swim bladders, indicating that the mutations are not larval lethal. Phenotypes at both loci are indistinguishable.

In *flycatcher*^{m370} the jaw phenotype is reminiscent of *pelican* and *grossmaul*. The eyes are however smaller and mutant embryos never inflate the swim bladder.

Other mutations affecting pharyngeal skeleton development

Several mutations were isolated that do not fit any of the above categories. Some of them are pleiotropic and are described in more detail along with their respective other phenotypes (see Table 1).

Mutant *captain hook*^{m169} embryos have a severely compressed and malformed pharyngeal skeleton. The ethmoid plate is absent (Fig. 7B).

The craniofacial phenotype of *maggot*^{m350} is reminiscent of members of group II (Fig. 7C), but *maggot*^{m350} is first detectable by its defect in notochord formation (Stemple et al., 1996). The cartilaginous structures are loosely packed and ill defined in their spatial extent.

Mutant *white bread*^{m384} embryos have a severe reduction in skeletal elements of the head (Fig. 7D). The ethmoid plate is formed but smaller. In some mutant embryos (about 10%) lower jaw structures do not stain with Alcian blue. In most mutants Meckel's cartilage and quadrate stain as very small and faint structures. Using DIC optics all skeletal elements can be identified, but are much smaller. Thus, the initial formation of the skeletal elements appears not to be affected. The phenotype remains similar at 8 dpf, with the exception that Meckel's cartilage, quadrate and ceratohyal stain slightly darker. There are no changes in the expression patterns of *krx-20*, *pax b*, *hlx-1* and *dlx* genes. *white bread*^{m384} complements all members of group I.

Skeletal analysis of *brak*^{m452} mutants reveals that all structures of the pharyngeal skeleton are formed but individual elements are bent to various degrees (Fig. 7E).

DISCUSSION

During a systematic genetic screen in zebrafish we have identified mutations in 34 loci affecting craniofacial development. The fact that only a single allele has been found for 26 out of the 34 loci, indicates that our screen has not approached saturation (see also Driever et al., 1996). Additionally, our visual screen was designed to find rather dramatic abnormalities. Future screens, using DIC optics, or markers like Alcian blue staining, will recover mutations with more subtle phenotypes. Similarly, interesting craniofacial abnormalities appearing as part of a pleiotropic phenotype might have gone unnoticed without the application of cartilage stains.

We did not attempt to recover mutations involved in ossification. Our screening procedure involving dissecting microscope inspection, as well as the time frame of evaluation, was insufficient to accurately reveal abnormalities in early bone formation.

No obvious defects have been observed in the axial skeleton of the trunk and tail. At the time of our staining procedure (5 dpf), no cartilaginous structures of the trunk and tail are stained by Alcian blue. Although the whole body axis of the mutants affected in chondrogenesis is shorter, the number and the shape of the somites appear to be normal.

Mutations affecting the layout of the pharyngeal skeleton

We characterized one group of mutants in which specific elements of the pharyngeal skeleton are absent or displaced. We have corroborated our results by detailed observation under the compound microscope, using DIC optics. We cannot exclude with certainty, however, that a structure scored as missing is simply not stained or inconspicuously small. The identity of skeletal elements was assigned by shape and position. Mutations might lead to misidentification of skeletal elements due to changes in shape or skeletal transformations. With these limitations in mind, we reasoned that the phenotypes observed in this group could result from defects in neural crest cell specification or migration.

Monitoring genes expressed in specific regions of the rhombencephalon at early somite and pharyngula stages as markers we did not detect differences in expression pattern between wild-type and mutant embryos. We therefore conclude that the overall organization of the rhombencephalon is not affected in these mutants. Specification problems in individual rhombomeres would be undetected by these assays. More detailed studies will have to be performed to rule out more subtle defects in rhombencephalic organization.

In order to assess the formation of the pharyngeal arch primordia, we analyzed the expression pattern of genes expressed by the immigrating neural crest cells and/or in adjacent cells of the pharyngeal arches (Akimenko et al., 1994). Again, no clear abnormalities in the expression pattern of these genes were ever observed. This is also true for the endodermal pouches of the pharyngeal arches.

The mutations affecting the layout of the pharyngeal skeleton likely affect the subsequent differentiation of the

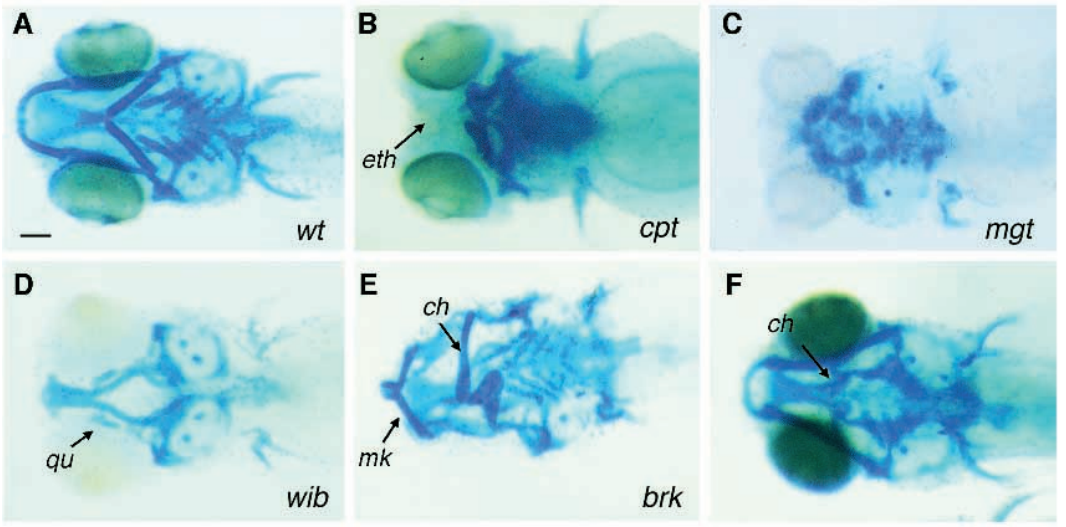

Fig. 7. Ventral view of Alcian blue stained day-5 mutant embryos, that have not been assigned to any of the three groups. (A) Wild-type. (B) *captain hook*^{m169}. (C) *maggot*^{m350}. (D) *white bread*^{m384}. (E) *brak*^{m452}. (F) An example of a mutant that was initially characterized as having a non-specific delay in development. Alcian blue staining reveals that the ceratohyal is malformed and does not reach the midline. ch, ceratohyal; eth, ethmoid plate; mk, Meckel's cartilage and qu, quadrate. Scale bar, 100 μm.

chondrogenic neural crest cells in a region-specific way but not the initial formation of the pharyngeal arches.

Expression and mutational studies have implicated Hox genes in patterning of the branchial region (Hunt and Krumlauf, 1992). These genes have sharp anterior borders of expression which coincide with rhombomere boundaries (reviewed by Hunt et al., 1991). In general, cranial neural crest cells emigrating from the rhombencephalon retain the Hox expression pattern of their original rhombencephalic origin. This pattern is unaltered, at least in rostrally transposed rhombomeres, even after transplantation to ectopic sites within the hindbrain (Guthrie et al., 1992; Kuratani and Eichele, 1993; Prince and Lumsden, 1994; Grapin-Botton et al., 1995) Mice with a disruption of the *hoxa-2* gene exhibit multiple cranial skeletal defects. Second pharyngeal arch-derived skeletal elements are absent in these mutants due to their transformation into more anterior structures (Gendron-Maguire et al., 1993; Rijli et al., 1993). Mice carrying a deletion of the *hoxa-3* gene are deficient in neural crest-derived structures. Craniofacial defects include altered shape and size of the mandible, neck cartilage and the absence of the lesser horn of the hyoid. In addition, they have severely deficient, or are missing, a thymus and thyroid, and parathyroid glands. Their heart and major blood vessels are also malformed (Chisaka and Capecchi, 1991). The migration of neural crest cells appears to be unaffected in mice deficient in *hoxa-3* (Manley and Capecchi, 1995). Double mutants defective in the paralogous genes *hoxa-3* and *hoxd-3* have more extensive skeletal defects than the combination of the phenotypes. This has been interpreted in a model in which Hox genes differentially regulate the proliferation rate of chondrogenic cells (Condie and Capecchi, 1993).

The phenotypes that we observe in our group I layout mutations are consistent with the involvement of these genes in regulating the expression or downstream effects of Hox genes. Similar to the mouse mutations, specific elements of the pharyngeal arches are malformed without a deficit in neural crest migration.

An alternative explanation is given by a time-boundary model. In the wild-type embryos, the pharyngeal skeleton develops roughly in an anterior-posterior sequence, with the exception of ceratobranchial V, which develops at about the same time as ceratobranchial I (Kimmel et al., 1995). A common aspect of the pharyngeal skeletal phenotypes in this group is that rostral elements (mandibular and hyoid elements) are less likely to be affected than more caudal elements (gill arch elements), with the exception of the ceratobranchial V. According to this model the given mutation causes a time-dependent block; that is cartilage forming before the block will differentiate whereas cartilage that would normally form after the block does not.

Mutations affecting cartilage formation and morphogenesis

We isolated a group of mutations that are likely to be affected in chondrogenesis. Mutations in this group are characterized by abnormal head morphology, smaller jaw structures, ear defects and a general reduction in body size. Skeletal analysis revealed that all elements of the pharyngeal skeleton are initially laid down but then fail to differentiate into proper cartilage bars. We postulate that mutations in this group are not affected in neural crest cell migration or the initial formation of the pharyngeal arches, but rather in chondrogenesis. In order to distinguish between a general delay in cartilage formation and a specific interruption in the chain of events leading to cartilage formation, we analyzed the pharyngeal skeleton in most mutations at stages of development later than 5 dpf. We did not observe a further progression in cartilage formation, arguing against a mere delay in chondrogenesis.

Following the establishment of the pharyngeal arches, chondrogenesis is initiated in chondrogenic neural crest cells. The first morphological sign is aggregation of mesenchymal cells. These condensations form the rough outline of the prospective skeletal elements. Subsequently the condensed cells will elaborate an extracellular matrix and differentiate into cartilage. Strong candidates for signaling molecules in cartilage formation are the bone morphogenetic proteins (BMP). They were originally isolated by virtue of their ability to induce bone formation at ectopic sites (Rosen and Thies, 1992). In two characterized mouse mutations cartilage condensation is affected. Mice homozygous for the *short ear* (*se*) and the *brachypodism* (*pb*) mutations have multiple skeletal

abnormalities (Lynch, 1921; Green and Green, 1942; Landauer, 1952). The mutations are in the genes encoding BMP-5 and GDF-5 (growth and differentiation factor 5) respectively; both molecules are members of the TGFβ superfamily (Kingsley et al., 1992; Storm et al., 1994).

Apart from skeletal defects, most members of this group fail to form semicircular canals of the inner ear. In wild-type embryos, the canals are formed by three paired axial projections into the lumen of the otic vesicle that eventually fuse at around 64 hpf (Waterman and Bell, 1984). In homozygous mutant embryos the projections are initially formed but fail to extend and fuse (Figure 4). This phenotype is similar to alterations seen after the injection into the otic vesicle of agents that interfere with the extracellular matrix (Haddon and Lewis, 1991; Gerchman et al., 1995). Therefore, abnormalities in semicircular canal formation may be due to a deficit in the extracellular matrix. These findings are consistent with the reduction of Alcian blue stain intensity. Alcian blue stains carbohydrate moieties on proteoglycans of the extracellular matrix. A failure of chondrogenic cells to differentiate or defects in genes encoding extracellular matrix components could result in the formation of a deficient or incomplete extracellular matrix.

A deficiency in aggrecan, a major cartilage specific proteoglycan core protein, has been shown to be causal in *nanomelia*, a recessive embryonic lethal mutation in chicken (Li et al., 1993). The phenotype of nanomelic chick embryos is similar to some of the mutations described here, with regards to their skeletal defects and the hypoplasia of the limbs. In mice the *cartilage matrix deficiency* (*cmd*) mutations produces a deletion in the aggrecan gene, leading to a similar phenotype (Watanabe et al., 1994).

Mutations affecting other aspects of craniofacial development

Another aspect of craniofacial development concerns the mechanical properties of the formed cartilaginous skeleton. This process might be affected in homozygous *brak*^{m452} embryos, where the pharyngeal skeleton is properly laid down and appears to be differentiated into cartilage bars. Individual elements however are bent to various degrees. This could be explained by a deficit in mechanical stability of the cartilage bars with the observed malformations resulting from mechanical stress.

An additional aspect of the formation of the pharyngeal skeleton is its proper connections to other tissues in the head. In order to function, the jaw apparatus needs to be connected to various muscles via tendons. We identified a group of mutations that affect the spatial arrangement of individual elements of the pharyngeal skeleton. It is conceivable that these mutations do not act on the skeletal elements themselves, but rather on their accessory structures.

Prospects

Our work initiates a genetic analysis of craniofacial development in zebrafish. The amenable genetics of zebrafish will make it possible to study genetic interactions among these genes and to find additional mutations. The optical properties of the zebrafish embryos will enable us to follow the assembly of the head skeleton and to study mutant phenotypes at the cellular level in vivo. The combination of both a genetic and embryological approaches will be fruitful for the study of tissue interactions during formation of the head skeleton. The advances in zebrafish genome resources (Postlethwait et al., 1994; Knapik et al., 1996) will hopefully soon link genetic data obtained in zebrafish with molecular data obtained in other systems and help to elucidate the molecular nature of the mutations described in this study.

We thank Colleen Boggs, Jane Belak, Heather Goldsboro and Lisa Anderson for excellent technical assistance. We like to thank Eliza Mountcastle-Shah and Kendrick A. Goss for critical reading of the manuscript. We are especially indebted to Dr Chuck Kimmel for helpful comments on the manuscript. The following colleagues kindly provided us with cDNA clones: T. Jowett, S. Krauss, A. Fjose, and M.-A. Akimenko. This work was supported by NIH RO1-HD29761 and a sponsored research agreement with Bristol Myers-Squibb (to W. D.). Further support in form of fellowships came from EMBO and Swiss National Fund (to A. S.), Helen Hay Whitney Foundation (to D. L. S. and D. Y. S.) and the Damon Runyon - Walter Winchell Cancer Research Fund (to J. M.).

REFERENCES

Akimenko, M. A., Ekker, M., Wegner, J., Lin, W. and Westerfield, M. (1994). Combinatorial expression of three zebrafish genes related to distal-less: part of a homeobox gene code for the head. *J. Neurosci.* **14**, 3475-86.

Chisaka, O. and Capecchi, M. R. (1991). Regionally restricted developmental defects resulting from targeted disruption of the mouse homeobox gene hox-1.5. *Nature* **350**, 473-479.

Condie, B. G. and Capecchi, M. R. (1993). Mice with targeted disruption in the paralogous genes hoxa-3 and hoxd-3 reveal synergistic interactions. *Nature* **370**, 304-307.

Couly, G. F., Coltey, P. M. and Le Douarin, N. M. (1993). The triple origin of skull in higher vertebrates: a study in quail-chick chimeras. *Development* **117**, 409-429.

De Beer, G. R. (1937). *The Development of the Vertebrate Skull*. London: Oxford University Press.

Driever, W., Solnica-Krezel, L., Schier, A. F., Neuhauss, S. C. F., Malicki, J., Stemple, D. L., Stainier, D. Y. R., Zwartkruis, F., Abdelilah, S., Rangini, Z., Belak, J. and Boggs, C. (1996). A genetic screen for mutations affecting embryogenesis in zebrafish. *Development* **123**, 37-46.

Ekker, M., Akimenko, M. A., Bremiller, R. and Westerfield, M. (1992). Regional expression of three homeobox transcripts in the inner ear of zebrafish embryos. *Neuron* **9**, 27-35.

Fjose, A., Izpisua-Belmonte, J. C., Fromental-Ramain, C. and Duboule, D. (1994). Expression of the zebrafish gene hlx-1 in the prechordal plate and during CNS development. *Development* **120**, 71-81.

Gendron-Maguire, M., Mallo, M., Zhang, M. and Gridley, T. (1993). Hoxa-2 mutant mice exhibit homeotic transformation of skeletal elements derived from cranial neural crest cells. *Cell* **75**, 1317-1331.

Gerchman, E., Hilfer, S. R. and Brown, J. W. (1995). Involvement of extracellular matrix in the formation of the inner ear. *Dev. Dyn.* **202**, 421-432.

Grapin-Botton, A., Bonnie, M.-A., McNaughton, L. A., Krumlauf, R. and LeDouarin, N. M. (1995). Plasticity of transposed rhombomeres: Hox gene induction is correlated with phenotypic modifications. *Development* **121**, 2707-2721.

Graveson, A. C. and Armstrong, J. B. (1987). Differentiation of cartilage from cranial neural crest in the axolotl (*Ambystoma mexicanum*). *Differentiation* **35**, 16-20.

Green, E. L. and Green, M. C. (1942). The development of three manifestations of the *short ear* gene in the mouse. *J. Morph.* **70**, 1-19.

Guthrie, S., Muchamore, I., Kuroiwa, A., Marshall, H., Krumlauf, R. and Lumsden, A. (1992). Neuroectodermal autonomy of Hox-2.9 expression revealed by rhombomere transposition. *Nature* **356**, 157-159.

Haddon, C. M. and Lewis, J. H. (1991). Hyaluronan as a propellant for epithelial movement: the development of semicircular canals in the inner ear of *Xenopus*. *Development* **112**, 541-550.

Hunt, P. and Krumlauf, R. (1992). *Hox* codes and positional specification in vertebrate embryonic axes. *Ann. Rev. Cell Biol.* **8**, 227-56.

Hunt, P., Whiting, J., Muchamore, I., Marshall, H. and Krumlauf, R. (1991). Homeobox genes and models for patterning the hindbrain and branchial arches. *Development* **Supplement 1**, 187-196.

Kelly, W. L. and Bryden, M. M. (1983). A modified differential stain for cartilage and bone in whole mount preparations of mammalian fetuses and small vertebrates. *Stain Technology* **58**, 131-134.

Kimmel, C. B., Ballard, W. W., Kimmel, S. R., Ullmann, B. and Schilling, T. F. (1995). Stages of embryonic development of the zebrafish. *Dev. Dyn.* **203**, 253-310.

Kingsley, D. M., E., B. A., Grubber, J. M., Marker, P. C., Russell, L. B., N.G., C. and Jenkins, N. A. (1992). The mouse *short ear* skeletal morphogenesis locus is associated with defects in a bone morphogenetic member of the TGFβ superfamily. *Cell* **71**, 399-410.

Knapik, E. W., Goodman, A., Atkinson, O. S., Roberts, C. T., Shiozawa, M., Sim, C. U., Weksler-Zangen, S., Trolliet, M. R., Futrell, C., Innes, B. A., Koike, G., McLaughlin, M. G., Pierre, L., Simon, J. S., Vilallonga, E., Roy, M., Chiang, P.-W., Fishman, M. C., Driever, W. and Jacob, H. J. (1996). A reference cross DNA panel for zebrafish (*Danio rerio*) anchored with simple sequence length polymorphisms. *Development* **123**, 451-460.

Krauss, S., Johansen, T., Korzh, V. and Fjose, A. (1991). Expression pattern of zebrafish pax genes suggests a role in early brain regionalization. *Nature* **353**, 267-270.

Kuratani, S. C. and Eichele, G. (1993). Rhombomere transplantation repatterns the segmental organization of cranial nerves and reveals cell-autonomous expression of homeodomain protein. *Development* **117**, 105-117.

Landauer, W. (1952). *Brachypodism*, a recessive mutation of house-mice. *J. Hered.* **43**, 293-298.

Langille, R. M. and Hall, B. K. (1987). Development of the head skeleton of the Japanese medaka *Oryzias latipes*. *J. Morph.* **193**, 135-158.

Langille, R. M. and Hall, B. K. (1988). Role of the neural crest in development of the cartilaginous cranial and visceral skeleton of the medaka, *Oryzias latipes* (Teleostei). *Anat. Embryol.* **177**, 297-305.

Le Douarin, N. M. (1982). *The Neural Crest*. Cambridge: Cambridge University Press.

Le Lievre, C. (1978). Participation of neural crest-derived cells in the genesis of the skull in birds. *J. Embryol. Exp. Morphol.* **47**, 17-37.

Li, H., Schwartz, N. B. and Vertel, B. M. (1993). cDNA cloning of chick cartilage condroitin sulfate (aggrecan) core protein and identification of a stop codon in the aggrecan gene associated with the chondrodystrophy nanomelia. *J. Biol. Chem.* **268**, 23504-11.

Lumsden, A., Sprawson, N. and Graham, A. (1991). Segmental origin and migration of neural crest cells in the hindbrain region of the chick embryo. *Development* **113**, 1281-1291.

Lynch, C. J. (1921). *Short ears*, an autosomal mutation in the house mouse. *Am. Natur.* **55**, 421-426.

Malicki, J., Schier, A. F., Solnica-Krezel, L., Stemple, D. L., Neuhauss, S. C. F., Stainier, D. Y. R., Abdelilah, S., Rangini, Z., Zwartkruis, F. and Driever, W. (1996). Mutations affecting development of the zebrafish ear. *Development* **123**, 275-283.

Manley, N. R. and Capecchi, M. R. (1995). The role of *Hoxa-3* in mouse thymus and thyroid development. *Development* **121**, 1989-2003.

Miyake, T. and Hall, B. K. (1994). Development of in vitro organ culture techniques for differentiation and growth of cartilages and bones from teleost fish and comparisons with in vivo skeletal development. *J. Exp. Zool.* **268**, 22-43.

Mullins, M. C., Hammerschmidt, M., Haffter, P. and Nüsslein-Volhard, C. (1994). Large-scale mutagenesis in the zebrafish: in search of genes controlling development in a vertebrate. *Curr. Biol.* **4**, 189-202.

Noden, D. M. (1975). An analysis of the migratory behavior of avian cephalic neural crest cells. *Dev. Biol.* **42**, 106-130.

Noden, D. M. (1983). The role of the neural crest in patterning of avian cranial skeletal, connective, and muscle cells. *Dev. Biol.* **96**, 144-165.

Oxtoby, E. and Jowett, T. (1993). Cloning of the zebrafish krox-20 gene (krx-20) and its expression during hindbrain development. *Nucl. Acids Res.* **21**, 1087-95.

Postlethwait, J. H., Johnson, S. L., Midson, C. N., Talbot, W. S., Gates, M., Ballinger, E. W., Africa, D., Andrews, R., Carl, T., Eisen, J. S. et al. (1994). A genetic linkage map for the zebrafish. *Science* **264**, 699-703.

Prince, V. and Lumsden, A. (1994). Hoxa-2 expression in normal and transposed rhombomeres: independent regulation in the neural tube and neural crest. *Development* **120**, 911-923.

Rijli, F. M., Mark, M., Lakkaraju, S., Dierich, A., Dolle, P. and Chambon, P. (1993). A homeotic transformation is generated in rostral branchial region of the head by disruption of *Hoxa-2* which acts as a selector gene. *Cell* **75**, 1333-1349.

Rosen, V. and Thies, R. S. (1992). The BMP proteins in bone formation and repair. *Trends Genet.* **8**, 97-102.

Schilling, T. F. (1993). Cell Lineage and Mutational Studies of Cranial Neural Crest Development in the Zebrafish. PhD Thesis. University of Oregon, Eugene

Schilling, T. F. and Kimmel, C. B. (1994). Segment and cell type lineage restrictions during pharyngeal arch development in the zebrafish embryo. *Development* **120**, 483-494.

Seufert, D. W. and Hall, B. K. (1990). Tissue interactions involving cranial neural crest in cartilage formation in *Xenopus laevis* (Daudin). *Cell Diff. Dev.* **32**, 153-166.

Solnica-Krezel, L. and Driever, W. (1994). Microtubule arrays of the zebrafish yolk cell: organization and function during epiboly. *Development* **120**, 2443-2455.

Solnica-Krezel, L., Schier, A. F. and Driever, W. (1994). Efficient recovery of ENU-induced mutations from the zebrafish germline. *Genetics* **136**, 1401-1420.

Solnica-Krezel, L., Stemple, D. L., Mountcastle-Shah, E., Rangini, Z., Neuhauss, S. C. F., Malicki, J., Schier, A. F., Stainier, D. Y. R., Zwartkruis, F., Abdelilah, S. and Driever, W. (1996). Mutations affecting cell fates and cellular rearrangements during gastrulation in zebrafish. *Development* **123**, 67-80.

Stainier, D. Y. R., Fouquet, B., Chen, J.-N., Warren, K. S., Weinstein, B. M., Meiler, S., Mohideen, M.-A. P. K., Neuhauss, S. C. F., Solnica-Krezel, L., Schier, A. F., Zwartkruis, F., Stemple, D. L., Malicki, J., Driever, W. and Fishman, M. C. (1996). Mutations affecting the formation and function of the cardiovascular system in the zebrafish embryo. *Development* **123**, 285-292.

Stemple, D. L., Solnica-Krezel, L., Zwartkruis, F., Neuhauss, S. C. F., Schier, A. F., Malicki, J., Stainier, D. Y. R., Abdelilah, S., Rangini, Z., Mountcastle-Shah, E. and Driever, W. (1996). Mutations affecting development of the notochord in zebrafish. *Development* **123**, 117-128.

Storm, E. E., Huynh, T. V., Copeland, N. G., Jenkisn, N. A., Kingsley, D. M. and Lee, S. J. (1994). Limb alterations in *brachypodism* mice due to mutations in a new memebr of the TGF-β superfamily. *Nature* **368**, 639-643.

Trevarrow, B., Marks, D. L. and Kimmel, C. B. (1990). Organization of hindbrain segments in the zebrafish embryo. *Neuron* **4**, 669-679.

Watanabe, H., Kimata, K., Line, S., Strong, D., Gao, L. Y., Kozak, C. A. and Yamada, Y. (1994). Mouse cartilage matrix deficiency (cmd) caused by a 7 bp deletion in the aggrecan gene. *Nature Genet.* **7**, 154-157.

Waterman, R. E. and Bell, D. H. (1984). Epithelial fusion during early semicircular canal formation in the embryonic zebrafish, *Brachydanio rerio*. *Anat. Rec.* **210**, 101-114.

Westerfield, M. (1994). *The Zebrafish Book*. Eugene: University of Oregon Press.

(Accepted 8 January 1996)